

Autonomous Control Model for C+L Multi-band Photonic Switch System using Machine Learning

*Original*

Autonomous Control Model for C+L Multi-band Photonic Switch System using Machine Learning / Khan, Ihtesham; Tunesi, Lorenzo; Masood, Muhammad Umar; Ghillino, Enrico; Bardella, Paolo; Carena, Andrea; Curri, Vittorio.. - ELETTRONICO. - (2021). (Intervento presentato al convegno Asia Communications and Photonics tenutosi a Shanghai China nel 24–27 October 2021) [10.1364/ACPC.2021.T4A.163].

*Availability:*

This version is available at: 11583/2949527 since: 2022-01-13T08:38:39Z

*Publisher:*

Optica Publishing Group

*Published*

DOI:10.1364/ACPC.2021.T4A.163

*Terms of use:*

This article is made available under terms and conditions as specified in the corresponding bibliographic description in the repository

*Publisher copyright*

Optica Publishing Group (formely OSA) postprint/Author's Accepted Manuscript

“© 2021 Optica Publishing Group. One print or electronic copy may be made for personal use only. Systematic reproduction and distribution, duplication of any material in this paper for a fee or for commercial purposes, or modifications of the content of this paper are prohibited.”

(Article begins on next page)

# Autonomous Control Model for C+L Multi-band Photonic Switch System using Machine Learning

Ihtesham Khan<sup>(1)</sup>, Lorenzo Tunesi<sup>(1)</sup>, M Umar Masood<sup>(1)</sup>, Enrico Ghillino<sup>(2)</sup>,  
Paolo Bardella<sup>(1)</sup>, Andrea Carena<sup>(1)</sup>, Vittorio Curri<sup>(1)</sup>,

<sup>(1)</sup> Politecnico di Torino, Corso Duca degli Abruzzi, 24, 10129, Torino, Italy;

<sup>(2)</sup> Synopsys, Inc., 400 Executive Blvd Ste 101, Ossining, NY 10562, United States

*ihatesham.khan@polito.it*

**Abstract:** We propose a data-driven technique for autonomous management of  $N \times N$  photonic switching systems in a software-defined networking setup. This work aims to demonstrate the C+L multi-band switching system and proposes a softwarized model for control. © 2022 The Author(s)

## 1. Introduction

The current intense increase of global Internet traffic and the new evolving concepts of the Internet of Things (IoT) demand an increase in optical networks' capacity and require a more flexible and dynamic network operating system at each layer. The majority of the present-day deployed optical transport networks exploits Wavelength-division multiplexing (WDM) across a spectral window of  $\approx 4.8$  THz in the C-band, with a transmission capacity of up to 38.4 Tb/s/fiber [1]. Additional expansion in the network capacity entails the implementation of different solutions, such as exploiting the residual capacity of already installed infrastructure or deploying new infrastructure. The initial solution, exploiting the residual capacity of already installed infrastructure, is more important for the network operator from a techno-economic perspective. In this regard, technologies such as Band-Division Multiplexing (BDM) is emerged as a promising solution to expand the capacity of existing WDM optical systems over the entire low-loss spectrum of optical fibers (e.g.,  $\approx 54$  THz in ITU G.652.D fiber) [2]. In addition to this, implementing the Software-Defined Network (SDN) paradigm provides the required degree of flexibility by virtualizing the network elements and functions within the network operating system. With the emergence of technologies such as coherent optical systems for WDM optical transport and re-configurable optical switches for transparent wavelength routing, in optical networking, the applications of the SDN paradigm can be extended down to the physical layer [3, 4]. For the implementation of SDN down to the physical layer, optical network components and transmission functionality must be abstracted for Quality-of-Transmission (QoT) impairments and for control to empower complete management by a single optical network controller [5, 6].

Nowadays, most optical network components, especially next-generation photonic switches, widely use Photonic Integrated Circuits (PICs) due to their low power consumption, lower latency, and small footprint. These PIC-based photonics switches rely mainly on the principle that the flow of light can be maneuvered by  $2 \times 2$  electrically controlled elements, like Mach-Zehnder (MZ) interferometers [7] or optical Microring Resonators (MRRs) [8]. In order to achieve a higher-order  $N \times N$  circuit, these elements are placed in more complex multi-stage topologies, which can achieve different routing properties depending on the chosen structure. The routing state is controlled through appropriate electrical signals provided to the element of the network structure. The deployment of this  $N \times N$  photonic switching system in the core optical networks and data centers mainly relies on its scalability factor. The key parameter for  $N \times N$  photonic switches' scaling is efficiently calibrating the internal control/routing states. The existing literature incorporates numerous deterministic routing algorithms to efficiently determine the internal switches' control state for any requested output permutation. These algorithms' effectiveness mainly relies on their topology dependency, enabling a faster and efficient assessment of the multistage networks. On the contrary, general-purpose routing algorithms do not deliver scalable solutions, as the computational complexity surges intensively [9, 10]. This complexity is triggered by the exponential increase of the control states  $N_{st}$  in the network, which depends on the number of Optical Switching Elements (OSE) as  $N_{st} = 2^{\text{OSE}}$ .

In opposite with conventional topology-dependent approaches, we present a unique topological and technological agnostic *blind* approach which exploits a Machine Learning (ML) method to model the control states of the  $N \times N$  photonic switch, which operates in a C+L multi-band. The ML engine is trained using a dataset obtained by the component with an arbitrary and potentially unknown internal structure in a complete black-box scenario. The suggested method is implemented in the context of an SDN: we introduce the concept of autonomous and software-based management of any C+L multi-band PIC-based optical switching system depicted in Fig. 1a.

## 2. Multi-band Switching System

In the implementation scenario under analysis, the switching structure is required to route all possible permutations of the  $N$  input signals while maintaining a wide-band range to support operation in the C+L transmission windows.

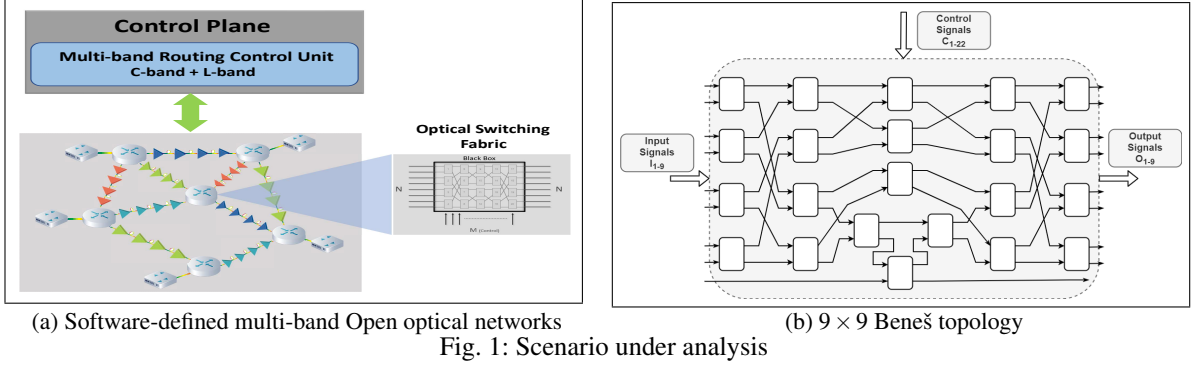


Fig. 1: Scenario under analysis

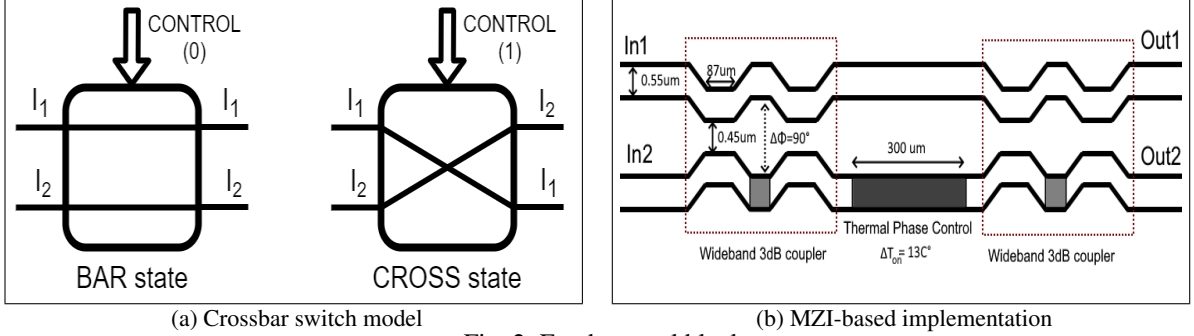


Fig. 2: Fundamental block

In order to allow scalability and reduce the overall footprint of the device, multistage switching structures are a commonly exploited solution. The elementary OSE must act as a  $2 \times 2$  CrossBar switch, depicted in Fig. 2a: the control signal  $C$  changes the configuration of the device between the BAR state ( $[I_1, I_2] \rightarrow [I_1, I_2]$  for  $C = 0$ ) and the CROSS state ( $[I_1, I_2] \rightarrow [I_2, I_1]$  for  $C = 1$ ). Due to the MRR narrow-band limitations [11], the device has been implemented through an MZI solution (Fig. 2b): the C+L operational range is provided by the wideband 3dB coupling structures, which allow low loss and dispersion compensation, while the device control is obtained through thermal tuning of one of the arms of the MZI, allowing the device to operate in both BAR and CROSS configuration.

The device performance has been simulated through the Synopsys Photonic Design Suite, with both material and transmission simulation in RSoft<sup>TM</sup> and Optisim<sup>TM</sup> [12]. The proposed OSE can achieve ultra-low losses in the whole bandwidth, as shown in Fig. 3, with the worst configuration being the BAR state (Fig. 3a) with less than 0.1dB of signal loss at the boundary of the C+L window.

In order to allow the routing of all input signals permutations, defined as the “non-blocking” property of a multistage topology, the designed OSE is placed in a Beneš network [13]. These structures are widely implemented due to their two main advantages: full routing possibility for every target permutation and small footprint; as a result, they reduced the number of operating OSEs with respect to other topologies. In this context, Fig. 1b shows the internal structure of a  $9 \times 9$  Beneš structure, which is made of  $M = 22$  elementary MZI cells: by properly piloting the control signals  $M_{1-22}$  every permutation of the input space ( $[I_1, I_2, \dots, I_9]$ ) can be obtained at the output stage ( $[O_1, O_2, \dots, O_9]$ ).

### 3. Dataset Generation & Machine Learning Model

The training and testing dataset for developing cognition in the ML engine is generated against the proposed  $9 \times 9$  Beneš structure. A subset of the overall  $2^M$  control combinations are exploited to produce a dataset stated in Tab. 1. The generated dataset is used to train a supervised neural network in the learning phase. The ML engine manages a *Deep neural network* (DNN), built by using the TensorFlow<sup>®</sup> library consists of *three* hidden-layers. The developed DNN model exploited *ReLU* as an activation function and mean square error (MSE) as a loss function. The proposed model is tuned with training steps of *1,000* and a learning rate of *0.01*. The training and testing subsets have a ratio of 70% and 30% of the generated dataset, described in Tab. 1. Moreover, the proposed ML engine manages wavelengths at the output ports as features and  $M$  control signals as labels.

Table 1: Dataset and ML Statistics

Beneš size $N \times N$	Permutations $N!$	Number of OSE	Combinations $2^M$	Dataset	Train Set	Test Set	Hidden-layers	Neurons per hidden-layer
$9 \times 9$	362,880	22	4,194,304	200,000	140,000	60,000	3	30

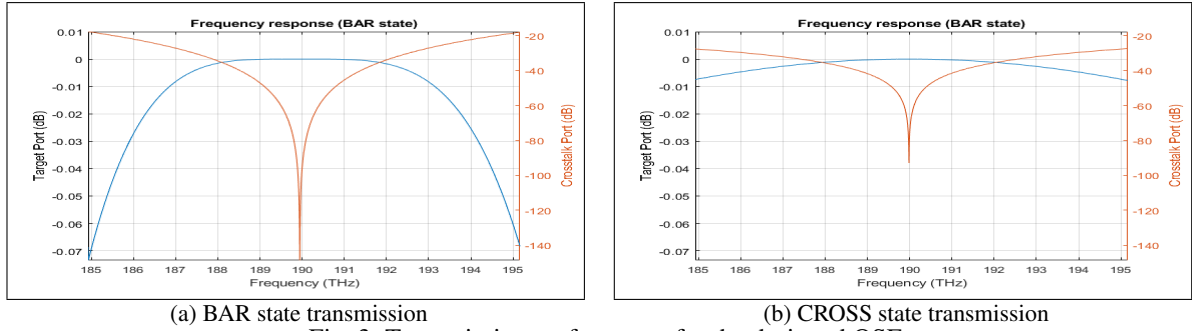


Fig. 3: Transmission performance for the designed OSE

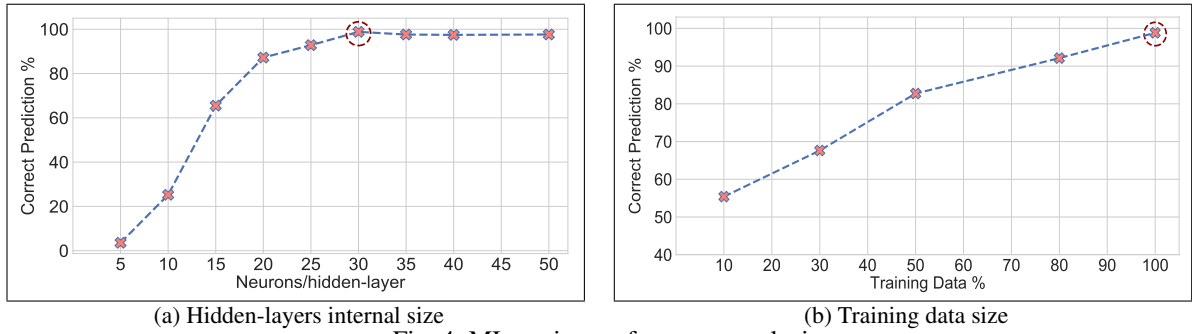


Fig. 4: ML engine performance analysis

#### 4. Results and Conclusion

The result section primarily demonstrates the influence of various ML parameters on the accuracy of predicting the control states of the C+L multi-band  $N \times N$  photonic switch. Fig. 4a shows the increasing number of neurons per hidden-layer vs. the progress in ML prediction ability. The increasing trend in prediction accuracy is observed to a specific point indicated by a circle; after that, an almost flat behavior is detected. Further, in Fig. 4b, the effect of the total considered training data size reported in Tab. 1 is also shown. The trend indicates that the prediction ability of the ML model increases with the growing training data size. Excellent results are achieved with the considered Beneš architecture (level of accuracy  $>98\%$ ). To further improve the prediction ability of the ML cognitive engine, an additional phase based on a simple heuristic is added that is mainly acquired from examining wrong configurations. Most of the errors in the prediction of the control state are due to a single OSE in the wrong state. The heuristic we propose tries to correct single OSE errors by flipping the control of one OSE during a single iteration and compares the output sequence vs. the desired output. The proposed heuristic further enhanced the predicting ability of the ML engine (level of accuracy improved to 100%).

In conclusion, we showed that a ML based approach could efficiently define the control states for a generic C+L multi-band  $N \times N$  photonic switch without knowing its topological details. Promising results in terms of high accuracy ( $>98\%$ ) are achieved with a limited size dataset using ML engine, which is further enhanced to 100% by applying a simple heuristic in real-time.

#### References

1. J. Pedro *et al.*, "Optical transport network design beyond 100 Gbaud," *JOCN* **12**, A123–A134 (2020).
2. A. Ferrari *et al.*, "Assessment on the achievable throughput of multi-band ITU-T G.652.D fiber transmission systems," *JLT* **38**, 4279–4291 (2020).
3. C.-S. Li *et al.*, "Software defined networks," *IEEE Commun. Mag.* **51**, 113–113 (2013).
4. M. Jinno *et al.*, "Elastic and adaptive optical networks: possible adoption scenarios and future standardization aspects," *IEEE Commun. Mag.* **49**, 164–172 (2011).
5. V. Curri, "Software-defined WDM optical transport in disaggregated open optical networks," in *ICTON*, (2020), pp. 1–4.
6. I. Khan *et al.*, "Automatic management of  $N \times N$  photonic switch powered by machine learning in software-defined optical transport," *IEEE Open J. Commun. Soc.* **2**, 1358–1365 (2021).
7. K. Suzuki *et al.*, "Low-insertion-loss and power-efficient  $32 \times 32$  silicon photonics switch with extremely high- $\delta$  silica PLC connector," *JLT* **37**, 116–122 (2019).
8. Q. Cheng *et al.*, "Ultralow-crosstalk, strictly non-blocking microring-based optical switch," *Photonics Res.* **7**, 155–161 (2019).
9. M. Ding *et al.*, "Routing algorithm to optimize loss and IPDR for rearrangeably non-blocking integrated optical switches," in *CLEO: Applications and Technology*, (OSA, 2015), pp. JTh2A–60.
10. Q. Cheng *et al.*, "Silicon photonic switch topologies and routing strategies for disaggregated data centers," *IEEE JSTQE* **26**, 1–10 (2020).
11. X. Tu *et al.*, "State of the art and perspectives on silicon photonic switches," *Micromachines* **10** (2019).
12. <https://www.synopsys.com/photonic-solutions.html>.
13. C. Chang and R. Melhem, "Arbitrary size Beneš networks," *Parallel Process. Lett.* **07**, 279–284 (1997).